Journal of Zhejiang University SCIENCE
ISSN 1009-3095
http://www.zju.edu.cn/jzus
E-mail: jzus@zju.edu.cn

Experimental study of seismic cyclic loading effects on small strain shear modulus of saturated sands*

ZHOU Yan-guo (周燕国)†, CHEN Yun-min (陈云敏), HUANG Bo (黄 博)

(*Department of Civil Engineering*, *Zhejiang University*, *Hangzhou 310027*, *China*)

†E-mail: qzking@zju.edu.cn

Received Nov. 17, 2003; revision accepted Feb. 11, 2004

Abstract: The seismic loading on saturated soil deposits induces a decrease in effective stress and a rearrangement of the soil-particle structure, which may both lead to a degradation in undrained stiffness and strength of soils. Only the effective stress influence on small strain shear modulus G_{max} is considered in seismic response analysis nowadays, and the cyclic shearing induced fabric changes of the soil-particle structure are neglected. In this paper, undrained cyclic triaxial tests were conducted on saturated sands with the shear wave velocity measured by bender element, to study the influences of seismic loading on G_{max}. And G_{max} of samples without cyclic loading effects was also investigated for comparison. The test results indicated that G_{max} under cyclic loading effects is lower than that without such effects at the same effective stress, and also well correlated with the effective stress variation. Hence it is necessary to reinvestigate the determination of G_{max} in seismic response analysis carefully to predict the ground responses during earthquake more reasonably.

Key words: Cyclic loading, Seismic response analysis, Undrained cyclic triaxial test, Small strain shear modulus, Effective stress, Bender element, Soil-particle structure

doi:10.1631/jzus.2005.A0229 **Document code:** A **CLC number:** TU411.8; TU415; TU435

INTRODUCTION

Adequate information on dynamic soil properties, especially dynamic shear modulus and damping ratio, is essential for accurate computations of ground response and soil-structure interaction problems. Many experimental investigations carried out on sandy soils through resonant column test or improved cyclic triaxial test in early studies (Hardin and Richart, 1963; Hardin and Black, 1968; Drnevich and Richart, 1970; Seed and Idriss, 1971; Kokusho, 1980) showed that the small strain shear modulus G_{max} ($\gamma<10^{-5}$) was basically related to the mean principal stress σ'_m and void ratio e of the soil, as expressed by the well known Hardin and Richart equations taking the general form:

$$G_{max} = AF(e)(\sigma'_m)^n \quad (1)$$

In which A is an empirical constant reflecting soil fabric formed through various stress and strain histories; n is an empirically determined exponent, approximately equal to 1/2; σ'_m is mean effective confining pressure; e is void ratio and $F(e)$ is void ratio function, which is usually given by:

$$F(e) = (2.973 - e)^2 / (1 + e) \quad (2)$$

Although the Hardin and Richart equations have since undergone several adjustments (Hardin and Drnevich, 1972a; 1972b; Iwasaki and Tatsuoka, 1977; Hardin, 1978; Hardin and Blandford, 1989; Hryciw and Thomann, 1993), for cohesionless soils these

*Project supported by the National Natural Science Foundation of China (No. 10372089) and Provincial Department of Education, Zhejiang Province (No. 20010572), China

various expressions could be readily reduced to almost the same form, with the most widely used one for G_{max} determination in the past decades being Eq.(1), especially in site-specific dynamic response analysis with total stress method (Idriss and Seed, 1968) or effective stress method (Finn *et al*., 1976; 1977; Martin and Seed, 1979; Papadimitriou and Bouckovalas, 2002).

It is generally known that in total stress analysis, Eq.(1) is used to estimate the small strain shear modulus variation in different layers with depth of soil profiles as the initial modulus for nonlinear analysis. Besides this, in effective stress analysis Eq.(1) will also account for the stiffness degradation caused by the gradual reduction of effective stresses in a given layer during seismic shaking, by updating the initial modulus G_{max} at various time intervals so as to be consistent with the σ'_m during the same interval. Thus the small strain shear modulus G_{max} is the key parameter for predicting the dynamic response and behavior of soils both in total stress and effective stress analyses, since it degrades with the reduction of σ'_m and acts as the basis of secant shear modulus G evaluation corresponding to the dynamic shear strain at the existing constant confinement (Fig.1).

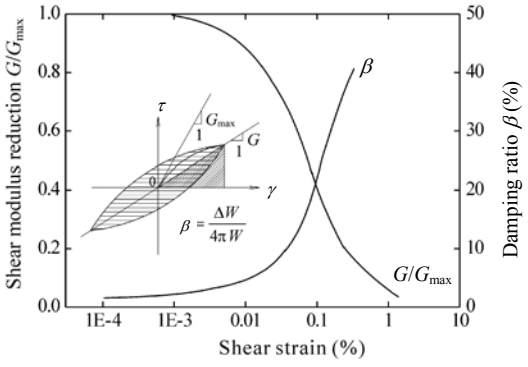

Fig.1 Nonlinear characteristics of soils (Martin and Seed, 1979)

However, it should be noted that Eq.(1) is summarized from the small strain (generally less than about 10^{-5}) measurement with static confinement in lab or in-situ, while during seismic shaking the soils behave dynamically and undergo relatively large shear strain (more than 10^{-3} in general), when the effective stress will decrease with the porewater pressures buildup due to plastic deformations in the soil skeleton, and therefore the loading effects on soils during earthquake are not the same as those reflected in Eq.(1). Vucetic (1994) found empirically that irreversible strains become increasingly significant for cyclic shear strain amplitude γ_c larger than the cyclic threshold shear strain γ_{tv}, which varies between 6.6×10^{-5} and 2.5×10^{-4} for nonplastic sands and silts. Evidently sand fabric (i.e., the orientation of particle contact planes) evolves during shearing. Hence directly assuming the small strain shear modulus G_{max} using Eq.(1) equal to that of sands during earthquake is not appropriate enough, and there is a necessity to examine more carefully the G_{max} of sands under cyclic loading.

To study the problems mentioned above, a piezoelectric-ceramic bender element measuring system was established using conventional cyclic triaxial apparatus, and a series of stress-controlled undrained cyclic triaxial tests were carried out on saturated sands with measured of shear wave velocity, to simulate the effects of seismic cyclic loading on soil stiffness, and investigate the variation mechanism of small strain shear modulus under this influence. The results of these tests indicated that G_{max} under the influences of cyclic loading was lower than that under no such influences at the same effective confinement, and well correlated with the effective stress and the soil fabric change factor.

EXPERIMENTAL STUDY

Test apparatus

To measure G_{max} of soils during undrained cyclic shearing, a piezoceramic bender elements system was established based on Model HX-100 multi-use triaxial apparatus (Huang *et al*., 2001). The test system frame is shown in Fig.2.

The bender element method was originally developed by Shirley and Anderson (1975) to obtain the very small strain shear modulus G_{max} of a soil by measuring the velocity of shear wave propagation through a sample, which has attracted intensive study since then (Shirley and Hampton, 1978; De Alba *et al*., 1984; Dyvik and Madshus, 1985; Thomann and Hryciw, 1990). A bender element is a piece of piezoceramic plate which bends if a voltage across it is changed or, if bent by an external force, the voltage

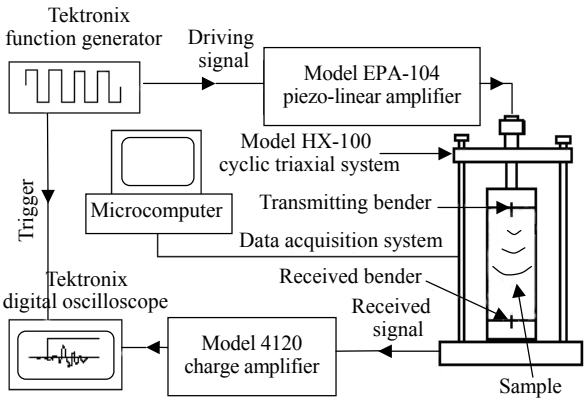

Fig.2 Schematic of triaxial system with bender element

across it changes. Bender elements are set into the top and bottom platens of a triaxial cell and penetrate about 3 mm into the sample (Fig.3). One element is vibrated by changing the voltage across it; shear waves propagate through the sample and vibrate the other element. The input and output voltages are continuously recorded and the travel time determined. The shear wave velocity V_s in the specimen can be calculated from the wave travel time t and the known separation L between the bender elements as

$$V_s=L/t \tag{3}$$

For a known material density ρ, according elastic theory, the small strain shear modulus can thus be calculated as

$$G_{\max}=\rho V_s^2 \tag{4}$$

Test procedures and contents

Saturated samples of 39.1 mm diameter and 80 mm height were sampled with the spooning method.

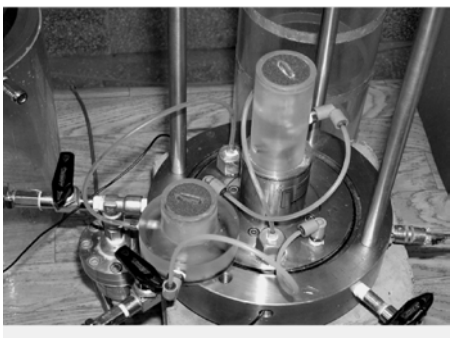

Fig.3 Triaxial cell equipped with bender element

The standard sand was angular grains crushed quartz with physical properties as given in Table 1.

Table 1 Fundamental properties of tested sands

Specific gravity G_s	Void ratio $e_{\max}$	Void ratio $e_{\min}$	Relative density D_r (%)	Grain size distribution		
				D_{10} (mm)	D_{50} (mm)	D_{90} (mm)
2.65	0.79	0.43	52~65	0.13	0.34	0.80

The mechanism of $G_{\max}$ of saturated sand under the influences of cyclic loading was investigated, and that of $G_{\max}$ without such influences was investigated for comparison. Comparison between the two series of tests will show the differences between them, and yield information on the influences of cyclic loading on small strain shear modulus.

Two ways were adopted to change the effective confining pressure of samples in tests without cyclic loading: (1) Samples were consolidated isotropically with effective confining pressure increasing gradually in steps of 0, 10, 25, 50, 75, 100, 150, 200, 250, 300 (kPa); (2) Samples were consolidated isotropically under high confining pressure first, then subjected to multi-stage backpressure with the effective stress decreasing gradually to zero. The backpressure tests were conducted in steps of 0, 100, 150, 200, 250, 300, 350, 375, 390, 400 (kPa). Shear wave velocity was measured after completion of consolidation at each loading stage.

The cyclic test procedure is illustrated in Fig.4. Samples were consolidated isotropically for 12 h at a given confinement and the shear wave velocity was measured for $G_{\max}$ before cyclic loading. Then they were subjected to a few number of uniform amplitude

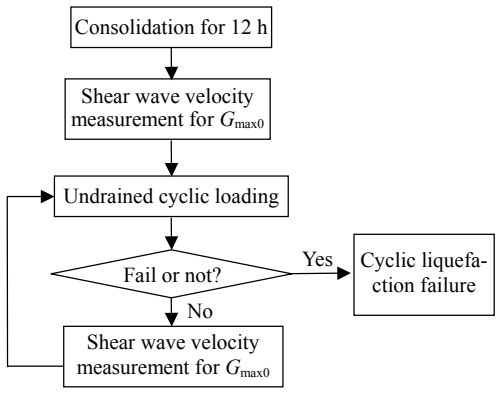

Fig.4 Cyclic test procedure flow chart

cyclic stresses at frequency of 1 Hz; and when the cyclic loading ended, the shear velocity for G_{max}, residual pore-water pressure and residual strain were recorded at the pause intervals only long enough to take reading (at about 1 min). This process was repeated throughout one test series until the cyclic failure occurred. The seven confining pressure levels selected for the tests were 50, 100, 150, 200, 250, 300, 400 (kPa), and spanned the range of soil pressure in-situ for seismic response analyses under normal circumstances. Meanwhile, several stress amplitudes were tried at a given confining pressure to check out the coincidence of test results with different "σ_d~N_l" combination, in which σ_d is cyclic stress amplitude, N_l is the accumulative cycle number of liquefaction failure.

TEST RESULTS AND ANALYSES

Preliminary test for determining the correct travel time

It is generally recognized that the principal thing with bender element method has always been the determination of the travel time t used to calculate V_s (Viggiani and Atkinson, 1995; Jovicic *et al*., 1996; Arulnathan *et al*., 1998). The travel time of an impulse wave between two points in a specimen may be taken as the time between the first direct arrival of shear wave at each point. To reduce the degree of subjectivity in the interpretation of t, several types of input signal and different frequencies for each signal were tried in preliminary tests, and the results with different travel time definition (S–A or S–B in Fig.5) were compared with those obtained from resonant column tests (Table 2), improving the confidence in the data. Resonant column tests were conducted by using Drnevich Long-Tor Apparatus.

As shown in Fig.5, the travel time values remained almost the same despite the exciting frequencies in (a) where the travel time is defined from S to A; but were relatively scattered in (b) where the travel time is defined as S–B. Further comparison in Table 2 shows that the shear modulus measured by bender element was a little higher than that obtained from resonant column tests for S–A travel time, but much lower for S–B travel time. Since the vibration shear strain amplitude in resonant column test was

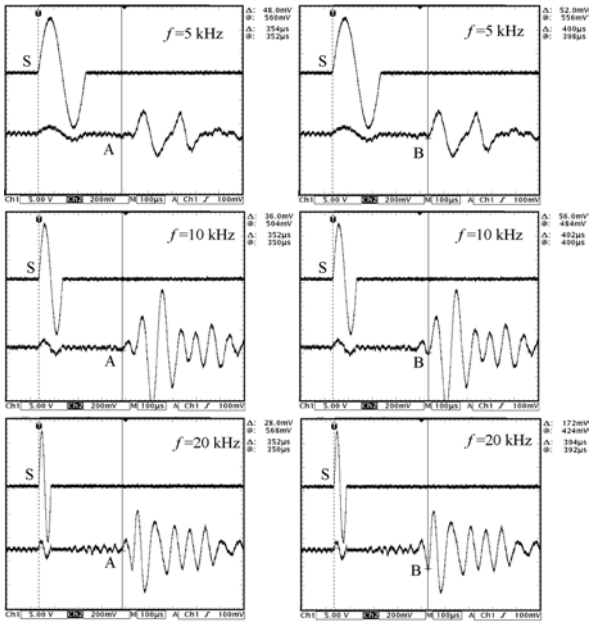

(a) (b)

Fig.5 Typical bender element traces (sine input) at confinement σ'_m=100 kPa

(a) Selected points (SP) for travel time: S–A; (b) Selected points (SP) for travel time: S–B

Table 2 Comparison between bender elements tests and resonant column tests

σ'_{m0} (kPa)	Bender element tests						Resonant column tests			
	D_r (%)	SP	F (kHz)	Δt (μs)	V_s (m/s)	$G_{max}/F(e)$ (MPa)	D_r (%)	γ ($\times10^{-6}$)	V_s (m/s)	$G_{max}/F(e)$ (MPa)
100	57.4	S–A	5	354	198.5	21.9	58.0	5.1	197.6	21.6
		S–A	10	352	199.6	22.1				
		S–A	20	352	199.6	22.1				
		S–B	5	400	175.4	17.1				
		S–B	10	402	174.5	16.9				
		S–B	20	394	178.1	17.6				
200	62.8	S–A	10	296	236.1	30.3	61.2	7.4	234.6	30.1
300	59.6	S–A	10	264	262.1	37.5	60.9	1.0	259.9	36.9

about 10^{-6}~10^{-5} and a bit higher than that in bender element (generally about 10^{-6} or less), it is reasonable to accept the S–A travel time as the correct travel time for about 10 kHz sine wave signal.

So in the subsequent tests, sine pulse was selected as the transmitted signal and the first reversal point A at the received trace was considered as the first arrival of the shear wave at the receiver bend element. Exciting frequencies selected were mainly about 10~15 kHz, but adjusted to lower values for low confinement such as σ'_m=25 kPa or higher values for higher confinement such as σ'_m=400 kPa to obtain the most explicit traces of receiver bender element.

Tests without cyclic loading effects

The test data on $G_{\max}$ versus the effective confining pressure σ'_m are plotted in Fig.6. To eliminate the influence of void ratio nonuniformity, $G_{\max}$ was further divided by $F(e)$ and the results are plotted in Fig.7, where e is the void ratio corresponding to the $G_{\max}$ at a given loading stage.

As shown in Fig.7, if divided by $F(e)$, the data points of the two test series are almost identical, and the small strain shear modulus $G_{\max}$ is well correlated with the effective stress σ'_m regardless of the void ratio. Then the fitting curve formula of them is given by

$$G_{\max} = 2.121 \cdot F(e)(\sigma'_m)^{0.505} \tag{5}$$

This results tally with those presented in previous study showing good correlation between $G_{\max}$ and σ'_m, e once again. In other words, in tests on sands under static confinement there was no significant effect of previous stress history and no evident effect of loading time was observed, and the small strain stiffness variations were mainly related to effective stress σ'_m and void ratio e changes.

Undrained cyclic triaxial tests

The test conditions of all the cyclic tests are listed in Table 3. And the small strain shear modulus

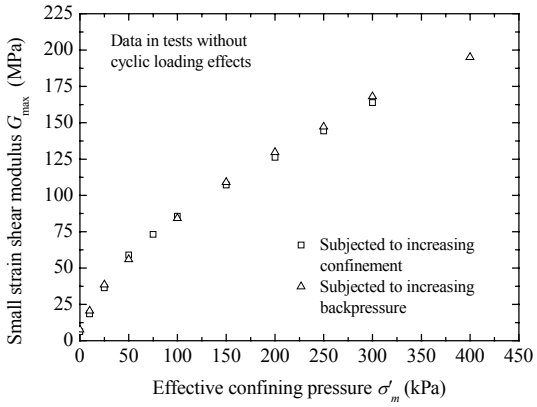

Fig.6 Variation of $G_{\max}$ with σ'_m

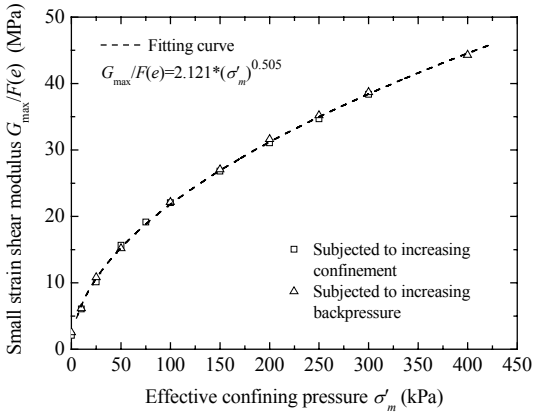

Fig.7 Variation of $G_{\max}/F(e)$ with σ'_m

Table 3 Test conditions of cyclic tests

Confining pressure σ'_{m0} (kPa)	Relative density D_r (%)	Cyclic stress amplitude σ_d (kPa)	Failure cycle number N_l	Confining pressure σ'_{m0} (kPa)	Relative density D_r (%)	Cyclic stress amplitude σ_d (kPa)	Failure cycle number N_l
150	55.4	51.3	38	100	54.9	31.5	15
150	52.3	38.5	108	100	57.8	21.0	575
150	55.1	26.5	1668	100	58.8	17.5	1229
200	59.9	56.0	43	300	62.1	83.0	115
200	62.8	44.0	479	300	59.6	59.8	713
200	65.0	37.0	2969	300	63.0	43.0	3581
250	52.8	66.0	68	50	58.8	18.0	531
250	56.0	68.5	210	400	55.0	90.6	188

G_{max} obtained at seven different confining pressures are plotted against effective stress σ'_m in Fig.8. There was similar trend of G_{max} variations with reduction of effective stress regardless of the confinement, and at each given confinement good agreement between different σ_d~N_l combinations (Table 3) could be seen.

As shown in Fig.9 with G_{max} divided by $F(e)$, besides the first point of each data group hitting almost the fitting curve of test data without cyclic loading effects, the other points are lower than the curve at the same effective stress: the former shows the variation of G_{max} without cyclic loading effects, while the latter reveals the characteristic of G_{max} influenced by cyclic loading. For explicitness, the modulus and effective stress are normalized by initial values G_{max} and σ'_{m0} respectively, and the results are plotted in Fig.10, where σ'_{m0} is the initial mean effective stress, due to the confinement; G_{max} is the initial small strain shear modulus before the porewater pressure generation.

If the small strain shear modulus without effects of cyclic loading is denoted as G^{I}_{max}, and the one under the influence of cyclic loading as G^{II}_{max}, the modulus difference $(G^{II}_{max}-G^{I}_{max})/G^{I}_{max}$ can be computed from data in Fig.10, with the results being plotted in Fig.11. Obviously the variation of G^{II}_{max} with effective stress reduction could be understood based on G^{I}_{max}, with further consideration of dynamic stresses induced rearrangement of soil-particle structure (macroscopically shown as the residual strain accumulation in Fig.12) effect on small strain shear modulus. It was not mere coincidence that as a measurement of fabric change in soil state after cyclic shearing, the G^{II}_{max} was well correlated with (σ'_m/σ'_{m0}), since the effective stress variation was mainly caused by the corresponding soil deformation characteristic (Finn *et al*., 1977; Martin and Seed, 1979), with the (σ'_m/σ'_{m0}) being somewhat of an ind-

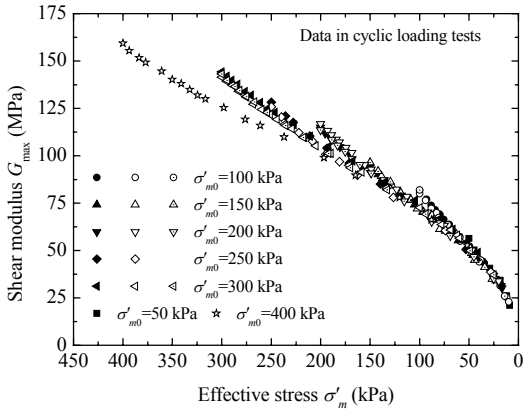

Fig.8 Original data of G_{max} versus σ'_m

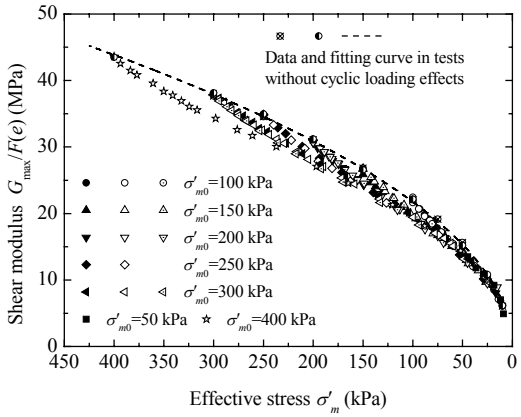

Fig.9 Variation of $G_{max}/F(e)$ with σ'_m

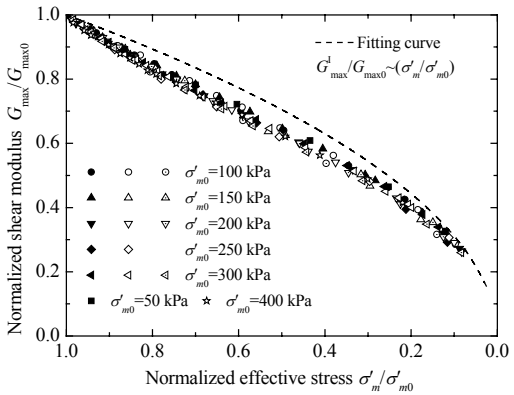

Fig.10 Variation of G_{max}/G_{max0} with σ'_m/σ'_{m0}

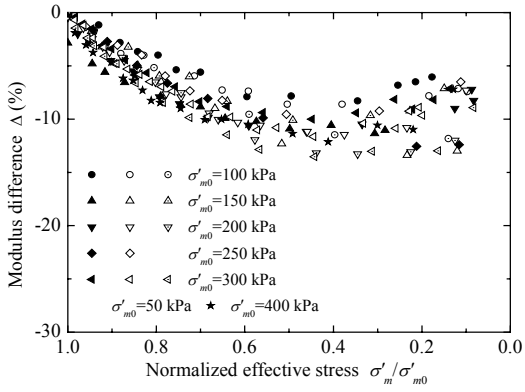

Fig.11 Variation of $(G^{II}_{max}-G^{I}_{max})/G^{I}_{max}$ with σ'_m/σ'_{m0}

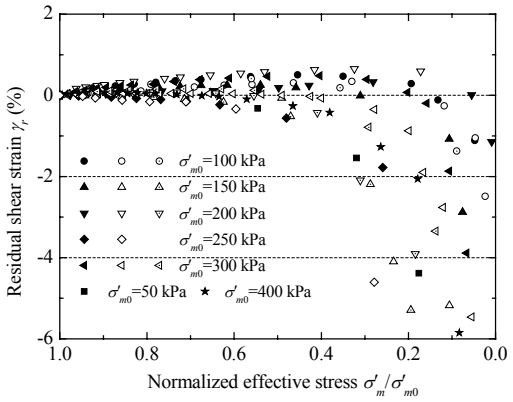

Fig.12 Residual shear strain γ_r versus σ'_m/σ'_{m0}

icator of soil fabric change under undrained conditions.

CONCLUSION

A series of undrained cyclic triaxial tests were conducted on saturated sands to simulate the influence of seismic cyclic loading on G_{max} of samples with and without cyclic loading effects. The test results indicated that:

1. The small strain shear modulus G_{max} under the cyclic loading effects is lower than that without such effects at the same effective stress. The modulus difference ($G^{II}_{max} - G^{I}_{max}$) appears at the beginning of cyclic shearing, increases with the effective stress reduction and reaches to more than 10 percent of G^{I}_{max}; then stabilizes or decreases slightly ultimately.

2. The G_{max} difference between the two types of test at the same effective stress was due to the influence of cyclic loading, which results in not only reduction of effective stress, but also the accumulation of interparticle contact slippage and grains connect crushing, namely, the rearrangement of soil-particle structure, which contribute to further reduction of G_{max}.

3. During earthquake, the ground deposit shakes continuously, so the determination of small strain shear modulus in seismic response analyses should take into account the cyclic loading effects, including both the induced effective stress reduction and rearrangement of the soil-particle structure. The test results presented here indicated that present seismic response analyses may overestimate the value of small strain shear modulus, which overestimation will increase with the development of earthquake process, thus the variety of response analysis results will be influenced to some extent. Therefore, it is necessary to carefully reinvestigate the determination of small strain shear modulus in present seismic response analyses and even to make some modification based on it.

ACKNOWLEDGEMENTS

The authors would like to acknowledge Ji Mei-xiu for his helpful suggestions on this study, and express their gratitude to Ma Yan-hong, Lin Wei-an and Yang Zhi for their kind help in conducting laboratory tests.

References

Arulnathan, R., Boulanger, R.W., Riemer, M.F., 1998. Analysis of bender element tests. *Geotechnical Testing Journal*, *ASTM*, **21**(2):120-131.

De Alba, P., Baldwin, K., Janoo, V., Roe, G., Celikkol, B., 1984. Elastic wave velocities and liquefaction potential. *Geotechnical Testing Journal*, *ASTM*, **7**(2):77-87.

Drnevich, V.P., Richart, F.E.Jr., 1970. Dynamic prestraining of dry sand. *Journal of the Soil Mechanics and Foundations Division*, *ASCE*, **96**(2):453-469.

Dyvik, R., Madshus, C., 1985. Laboratory Measurement of G_{max} Using Bender Elements. Proceedings of ASCE Annual Convention: Advances in the Art of Testing Soils under Cyclic Conditions, Detroit.

Finn, W.D.L., Byrne, P.M., Martin, G.R., 1976. Seismic response and liquefaction of sands. *Journal of Geotechnical Engineering Division*, **102**(8):841-856.

Finn, W.D.L, Lee, K.W., Martin, G.R., 1977. An effective stress model for liquefaction. *Journal of the Geotechnical Engineering Division*, *ASCE*, **103**(6): 517-533.

Hardin, B.O., 1978. The Nature of Stress-strain Behavior for Soils. Conference on Earthquake Engineering and Soil Dynamics, ASCE, p.3-90.

Hardin, B.O., Richart, F.E.Jr., 1963. Elastic wave velocities in granular soils. *Journal of the Soil Mechanics and Foundations Division*, *ASCE*, **89**(1):33-65.

Hardin, B.O., Black, W.L., 1968. Vibration modulus of normally consolidated clay. *Journal of the Soil Mechanics and Foundations Division*, *ASCE*, **94**(2):353-369.

Hardin, B.O., Drnevich, V.P., 1972a. Shear modulus and damping in soils: measurement and parameter effects. *Journal of the Soil Mechanics and Foundations Division*, *ASCE*, **98**(6):603-624.

Hardin, B.O., Drnevich, V.P., 1972b. Shear modulus and damping in soils: design equations and curves. *Journal of the Soil Mechanics and Foundations Division*, *ASCE*, **98**(7):667-693.

Hardin, B.O., Blandford, G.E., 1989. Elasticity of particulate materials. *Journal of Geotechnical Engineering*, *ASCE*, **115**(6):788-805.

Hryciw, R.D., Thomann, T.G., 1993. Stress-history-based model for G^e of cohesionless soils. *Journal of Geotechnical Engineering*, *ASCE*, **119**(7):1073-1093.

Huang, B., Yin, J.H., Chen, Y.M., Wu, S.M., 2001. Measurements of elastic shear modulus G_{max} using piezoceramic bender elements. *Journal of Vibration Engineering*, **14**(2):155-160 (in Chinese).

Idriss, I.M., Seed, H.B., 1968. Seismic response of horizontal soil layers. *Soil Mechanics and Foundations Division*, *Proceedings of ASCE*, **94**(4):1003-1031.

Iwasaki, T., Tatsuoka, F., 1977. Effects of grain size and grading on dynamic shear moduli of sands. *Soils and Foundations*, **17**(3):19-35.

Jovicic, V., Coop, M.R., Simic, M., 1996. Objective criteria for determining G_{max} from bender element. *Geotechnique*, **46**(2):357-362.

Kokusho, T., 1980. Cyclic triaxial test of dynamic soil properties for wide strain range. *Soils and Foundations*, **20**(2): 45-60.

Martin, P.P., Seed, H.B., 1979. Simplified procedure for effective stress analysis of ground response. *Journal of the Geotechnical Engineering Division*, *ASCE*, **105**(6):739-758.

Papadimitriou, A.G., Bouckovalas, G.D., 2002. Plasticity model for sand under small and large cyclic strains: a multiaxial formulation. *Soil Dynamics and Earthquake Engineering*, **22**:191-204.

Seed, H.B., Idriss, I.M., 1971. Simplified procedure for evaluating soil liquefaction potential. *Journal of the Soil Mechanics and Foundation Division*, *ASCE*, **97**(9):1249-1273.

Shirley, D.J., Anderson, A.L., 1975. In situ measurement of marine sediment acoustical properties during coring in deep water. *IEEE Trans on Geoscience and Electronics*, **GE-13**(4):163-169.

Shirley, D.J., Hampton, L.D., 1978. Shear wave measurements in laboratory sediments. *Journal of the Acoustical Society of America*, **63**(2):607-613.

Thomann, T.G., Hryciw, R.D., 1990. Laboratory measurement of small strain shear modulus under K_0 conditions. *Geotechnical Testing Journal*, *ASTM*, **13**(2):97-105.

Viggiani, G., Atkinson, J.H., 1995. The interpretation of the bender element tests. *Geotechnique*, **45**(1):149-154.

Vucetic, M., 1994. Cyclic threshold shear strains in soils. *Journal of Geotechnical Engineering*, *ASCE*, **120**(12): 2208-2228.